

L-system tree model and LIDAR simulator: estimation of spray target area.

A M TARQUIS¹, V. MÉNDEZ¹, P J WALKLATE², M.T. CASTELLANOS¹ and M.C. MORATÓ¹

¹ Dpto. de Matemática Aplicada a la Ingeniería Agronómica.

E.T.S. de Ingenieros Agrónomos - U.P.M.

Ciudad Universitaria s.n. 28040 Madrid.

SPAIN

²Silsoe Research Institute

Wrest Park, Bedford, MK45 4HS.

UNITED KINGDOM.

Abstract: - The ability to estimate the target area of row crops is an important requirement for the development, registration and efficient use of modern crop protection products for tree fruit spraying. In this study we simulated the LIDAR system using a trajectory model of light transmission compare estimates of the spray target area from LIDAR recordings. The branching structure and dimensional detail of typical tree-row targets is generated numerically using an open L-system model. The results show good correlation between the area estimates given by the simulation system and the records.

Key-Words: - measurement techniques, numerical simulation, L-systems model

1 Introduction

Since the commercial development of the first low-cost LIDAR system (Wangler et al., 1994), intended for feed-back sensing of trees during orchard spraying, this and similar systems have been used to record and quantify crop structural detail in support of pesticide applications research (Walklate et al., 1997; Walklate et al., 2000; Cross et al., 2001 a & b; Walklate et al., 2002; Cross et al., 2003; Walklate et al., 2003; Salyani & Wei, 2005; Sanz et al., 2005).

The purpose of this numerical study is to assess the accuracy of tree area estimation based on the LIDAR recording and post-processing methodology (Walklate et al., 2002). The functionality of the LIDAR sensing and recording process is simulated using a trajectory model (Tarquis & Mendez Fuentes, 2004) to determine light transmission through typical targets, assuming the back-scattered light is of sufficient intensity to exceed the detection threshold. The spatial structure of the target is generated numerically using an L-system model (Prusinkiewicz and Lindenmayer, 1990; Tarquis & González-Andrés, 1995). The study describes the modelling of row crops that are similar to the range of pre-blossom spray targets found in modern top fruit production in the UK.

2 Materials and Methods.

2.1 Tree model.

An open L-system model (Tarquis and González-Andrés, 1995) is used to produce a geometric description of the branching pattern for a typical pre-blossom tree structure. The model consists of an initial axiom (Fig. 1) and a set of production rules to characterise the cumulative effect of m generation cycles. In this L-system, three active buds are used to define the sites for generating the next axiom.

For the i^{th} generation cycle the following mathematical expressions define: the number of

branch elements $n_i = j k^{(i-1)}$ of length $l_i = \frac{L}{2^{(i-1)}}$

where L is the branch element length of the initial axiom. Furthermore, to simulate the detailed geometry of a tree structure, the stick-like branches shown in Fig 1 are replaced by cylinders of

diameter $d_i = \frac{2 m R}{i}$, where R is the minimum

branch radius. Examples of the tree-like structures that are the result of cumulative branch generation (i.e. $m=1, 3$ & 7) are shown for other variable inputs of: minimum branch radius (Fig 2), axiom rotation angle (Fig 3) and branching angle (Fig 4).

2.2 Estimate of target area for simulation of destructive sampling.

For this tree model the following expression is used to determining the cumulative branch area given by a methodology that combines destructive sampling of the tree and shadowgraph measurement of individual branches:

$$A_d = \sum_{i=1}^m d_i l_i n_i = \sum_{i=1}^m \left(\frac{2mR}{i} \right) \left(\frac{L}{2^{(i-1)}} \right) (jk^{(i-1)}) \quad (1)$$

This expression neglects the small modifications for intersection between non-orthogonal branches.

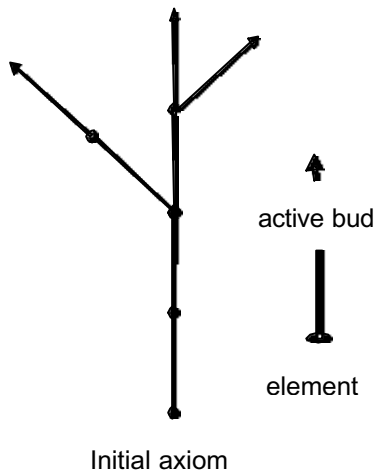


Fig.1. Initial axiom (i.e. generation $i=1$) of an L-system branching structure which is made up of $j=7$ elements and $k=3$ active buds (i.e. sites for generating the next axiom).

2.3 LIDAR simulation (SimLidar).

A trajectory model is used to simulate the scanning beam of the LIDAR system and determine the range and angle to the first point of interception with the target crop. Typical operational settings for this simulation are defined by: the scanning beam angular resolution of 0.5° , the spatial increment of 2 mm between consecutive scans and the axis of scanning at 1m above the ground and at 2m from the tree-row. For each rotational scan the LIDAR simulator produces a typical output sequence of 200 range measurements at trajectory angles between limits of -50.0° and $+50.0^\circ$ azimuth

2.3.1 3D Representation of the tree model.

The L-system with the wood structure of the apple tree, giving to SimLidar a file with all the branches attributes.

It is assumed that each branch is represented by a cylinder which is defined by the coordinated of the two extreme points; $(x_1 \ y_1 \ z_1)$ and $(x_2 \ y_2 \ z_2)$

that belong to the cylinder axes; and the cylinder radius r .

The set of branches; with these three parameters (two points and the radius), are the base of the file used by SimLidar.

SimLidar keeps in memory this information, a cylinder object in three dimensions (3D) are created by SimLidar (Cilindro3D).

The attributes of the Cilindro3D object are:

- Initial Point of the central axis (P1).
- Final Point of the central axis (P2).
- Radius (r).
- Contour.

SimLidar storage the points in a particular class of objects (CPunto3D), based on the vector position of the point (three coordinates). The type of variable in C++ that is used for each coordinate is float.

The Contour (Contorno3D of SimLidar) used is the cube with minimum volume that includes the cylinder. Each contour is defined by the minimum $(x_{\min} \ y_{\min} \ z_{\min})$ and a maximum of $(x_{\max} \ y_{\max} \ z_{\max})$ cube's coordinates.

SimLidar uses the contour to differentiate if any intersection occurs or not between two objects. For example, two Cilindro3D object can show an intersection if exist an intersection between their contours, otherwise that case is impossible. If that is the case, the intersection of the two cylinders is calculated through algebraic equations.

This fact is very useful to analysed a big set of objects and compare them two by two without losing precision in the calculations and saving computational time.

Meanwhile the branch set is loading and storage in the memory, the contour of the crop is calculated. In this way we obtained the coordinates of two corners of the cube, one of them correspond to the minimum values $(\text{Min}\{x\}, \text{Min}\{y\}, \text{Min}\{z\})$ and the other one to the maximum values $(\text{Max}\{x\}, \text{Max}\{y\}, \text{Max}\{z\})$.

The LIDAR system records the crop interception range distribution of all the orchard structures advancing for a traverse parallel to the tree row that is taken as the axis OY. The centre of the scanning axis is at a fixed height and the transmitter beam of the

system is perpendicular to the tree row (OX axis). A complete scanner with the LIDAR in a certain location (x_0, y_0, z_0) is done changing the angle from a minimum $(\text{Min}\{\theta\})$ to a maximum value $(\text{Max}\{\theta\})$ that assures to cover the crop. The advanced in the OY axis, a constant Δy , is realized after each scanner.

In each iteration y value is increased by a constant amount (Δy) . For an i^{th} iteration the y coordinate is:

$$y_i = y_1 + (i - 1) * \Delta y \quad (2)$$

$$i = 1 \dots N \text{ being } N = \text{Integer} \left(\frac{\text{Max}\{y\} - \text{Min}\{y\}}{\Delta y} \right)$$

N is the number of completed cycles done.

2.3.2 LIDAR angle variation

A complete cycle occurs when q varying from $\text{Min}\{q\}$ to $\text{Max}\{q\}$ with constant increments (Δq) . The q value at the k -th iteration is:

$$q_k = q_1 + (k - 1) * \Delta q \quad (3)$$

$$k = 1 \dots K \text{ being } K = \text{Integer} \left(\frac{\text{Max}\{q\} - \text{Min}\{q\}}{\Delta q} \right)$$

K represents the number of sub-samples for each cyclic. This value can be reduced calculating the minimum (q_1) and maximum (q_K) angle where it is possible to intersect the crop, given by the relations:

$$q_1 = -\arctan \left(\frac{z_0}{\text{Max}\{x\} - x_0} \right) \quad (4)$$

$$q_K = \arctan \left(\frac{\text{Max}\{z\} - z_0}{\text{Max}\{x\} - x_0} \right) \quad (5)$$

The total range samples are given by $K \times N$.

2.3.3 LIDAR angle scanner

In each simulated transmitter/receiver beam, SimLidar makes discrete radial displacements (Δr) from the origin (x_0, y_0, z_0) in a certain direction searching for the nearest branch. Then $K \times N$

number of searches with different directions will be done obtaining $K \times N$ radial distances.

The radial distance (r) can be calculated based on initial value (r_1) and the addition of the subsequent displacements (Δr) . At the j^{th} iteration the radial distance will be:

$$r_j = r_1 + (j - 1) * \Delta r \quad (6)$$

The initial value could be choosing as the first radial distance where an intersection with the crop is possible. Then, the r_1 value is:

$$r_1 = \frac{\text{Max}\{x\} - x_0}{\cos(q_k)} \quad (7)$$

Following the same logic, the maximum radial distance, achieved by J iterations (r_j) , will be calculated by the following expression:

$$r_j = \frac{\text{Min}\{x\} - x_0}{\cos(q_k)} \quad (8)$$

2.3.4 Intersection between crop and discrete local sampling volume

The LIDAR searching divides the total volume in discrete local volume $(\Delta y \cdot \Delta q \cdot \Delta r)$. With each sampling volume an intersection with a branch is studied.

Given a position (y_i) and a sampling angle (q_k) SimLidar study the geometric characteristics of each discrete local volume, varying the radial distance (r_j) between r_1 and r_j ($r_1 \leq r_j \leq r_j$), and compare with the crop objects.

The number of crop objects is equal to the number of branches (R) , and for each discrete local volume R computations are done to study the intersection. The first step is to observe if exists any intersection between the cubic contours of both objects.

The contour of a discrete local sampling volume $(\Delta y \cdot \Delta q \cdot \Delta r)$ will be found between the following coordinates:

$$\begin{aligned} z_1 &= z_0 + (r_j + \Delta r) * \sin(q_k) \\ z_2 &= z_0 + (r_j + \Delta r) * \sin(q_k + \Delta q) \end{aligned} \quad (9)$$

Finally from both values the minimum and maximum value will be attached to the minimum and maximum of the contour respectively.:

$$\begin{aligned} z_{\min} &= \text{Min}(z_1 \quad z_2) \\ z_{\max} &= \text{Max}(z_1 \quad z_2) \end{aligned} \quad (10)$$

In the same way, the extremes of the contour respect to axis OX are obtained:

$$\begin{aligned} x_1 &= x_0 + (r_j + \Delta r) * \cos(\mathbf{q}_k) \\ x_2 &= x_0 + (r_j + \Delta r) * \cos(\mathbf{q}_k + \Delta r) \end{aligned} \quad (11)$$

And the contour extremes are:

$$\begin{aligned} x_{\min} &= \text{Min}(x_1 \quad x_2) \\ x_{\max} &= \text{Max}(x_1 \quad x_2) \end{aligned} \quad (12)$$

The extreme values of the cubic contour respect to OY axis are:

$$\begin{aligned} y_{\min} &= y_i \\ y_{\max} &= y_i + \Delta y \end{aligned} \quad (13)$$

To study the precise intersection between the sampling and the branch (cylinder) a matrix of points are generated to represent the discrete local sampling. The methodology to select the points is explained above.

The determination of the point matrix is a function of an integer number (P) related to the precision, SimLidar assumes the value $P=2$. Therefore, the number of points that configured the matrix is $(P+1)^3$, and in the case of $P=2$ gives 27 points representing the discrete volume considered.

The coordinates can be represented as a cubic matrix of dimension $P+1$. The indexes of the matrix elements will be represented as a super index by a letter (a, b, c). Then, a generic element belonging to the point matrix is:

$$(x \quad y \quad z)^{a,b,c} = (x^{a,b,c} \quad y^{a,b,c} \quad z^{a,b,c}) \quad (14)$$

with $1 \leq a \leq P+1$, $1 \leq b \leq P+1$ and $1 \leq c \leq P+1$. Each one of the coordinates is:

$$x^{a,b,c} = x_0 + \left(r_j + (c-1) * \frac{\Delta r}{P} \right) * \sin \left(\mathbf{q}_k + (b-1) * \frac{\Delta \mathbf{q}}{P} \right) \quad (15)$$

$$y^{a,b,c} = y_i + (a-1) * \frac{\Delta y}{P} \quad (16)$$

$$z^{a,b,c} = z_0 + \left(r_j + (c-1) * \frac{\Delta r}{P} \right) * \cos \left(\mathbf{q}_k + (b-1) * \frac{\Delta \mathbf{q}}{P} \right) \quad (17)$$

Where $(x_0 \quad z_0)$ is the LIDAR origin of the axis. And where $\{ y_i \quad \mathbf{q}_k \quad r_j \}$ is the actual position of the searching.

Intersection between a cylinder and a crop object. Given a discrete volume sampling position $(y_i \quad \mathbf{q}_k \quad r_j)$ the cubic contour is defined by $(x_{\min} \quad y_{\min} \quad z_{\min})$ and $(x_{\max} \quad y_{\max} \quad z_{\max})$ and the point matrix as $(x^{a,b,c} \quad y^{a,b,c} \quad z^{a,b,c})$.

On the other hand, the contour of the branch is defined, as explained before, by $(x_{\min}^* \quad y_{\min}^* \quad z_{\min}^*)$ and $(x_{\max}^* \quad y_{\max}^* \quad z_{\max}^*)$ cube's coordinates.

The first step is to check if both contours are disjoint or not. If they are, it is impossible that an intersection happens between them. The case of disjoint will be concluded if any of the follow conditions happens:

$$\begin{aligned} x_{\min} &> x_{\max}^* & x_{\max} &< x_{\min}^* \\ y_{\min} &> y_{\max}^* & y_{\max} &< y_{\min}^* \\ z_{\min} &> z_{\max}^* & z_{\max} &< z_{\min}^* \end{aligned} \quad (18)$$

This allows us to discard those branches without any space in common with the discrete volume sample. In the opposite case, the possible intersection is calculated studying if any of the points representing the sample is an inset point to the cylinder.

This geometrical problem is resolved comparing the position of a point belonging to the matrix with:

- a) The two planes defined by the extremes point of the cylinder axis. These planes should be orthogonal to the axis.
- b) The radius of the cylinder. If the distance from the point to the cylinder axis is less or equal to the cylinder radius, beside the point is in between the two planes, the intersection has been found.

2.3.5. Result of LIDAR Index

Each position representing a discrete volume sampling is defined by q_k , the total amount of discrete volumes will be $N \times K$. The process will give us for each position the radial distance at which the intersection has been occurred, building a matrix (L) with $N \times K$ elements.

If the intersection with a branch is found in the j -th iteration of radial displacement the element $L(i, k)$ will have the value r_j being $r_1 \leq r_j \leq r_j$. Otherwise two cases are contemplated depending on the sign of q_k .

If $q_k < 0$ the beam will touch the soil, in other words the plane $z = 0$. The LIDAR index will have the value:

$$L(i, k) = \sqrt{\left(\frac{z_0}{\tan(-q_k)}\right)^2 + (z_0)^2} \quad (19)$$

If $q_k \geq 0$ not having an intersection with any branch the point escape to the infinite. The element of the matrix will have a tabulated number big enough (F) to differentiate from the rest of points and then $L(i, k) = F$

2.4 Estimate of target area from LIDAR recording

The method described by Walklate et al. (2002) is used to determine key tree-row parameters from LIDAR recordings given by the simulator. The calculation involves an intermediate data reduction step to compute the two-dimensional distribution of the target interception probability P . Thus, the classical tree-row parameters are defined in terms of the tree-row-cross-section, where $P \geq 1\%$. This is represented as the product $h b$, where the tree-row-height is h and the tree-row-width is b . The following expression therefore gives the target area of interception by a LIDAR traverse of length ℓ along the tree-row:

$$A_i = h b a \ell \quad (20)$$

where a is the area-density of the tree-row.

3 Results

Images of model trees are presented in Fig 2, 3 & 4 alongside the correlation between target area estimates derived from both LIDAR and destructive sampling methodologies. The correlation in Fig 2 shows variation in the origins of the log transformed data for simulations with different ranges of branch diameter (i.e. different values of minimum branch radius and number of generation cycles). This is indicative of the error that might be expected when the target trees contain a high proportion of branches that are inadequately resolved by the scanning beam of the LIDAR. Figs 3 & 4 show another manifestation of the same fundamental problem as the resolution of different branch elements is changed by perturbing the axiomatic rotation angle and vertical branching angle of the L-system tree model. For further details see [13].

4 Conclusion

The ability to estimate the target area of row crops is an important requirement for the development, registration and efficient use of modern crop protection products for tree fruit spraying. This study suggests that target area estimates from LIDAR systems, set-up for appropriate spatial resolution of the target, give good correlation with estimates based on destructive sampling. Further work is needed to establish a suitable indicator for the quality of tree area estimation from LIDAR recordings and examine the potential for correction based on similarity scaling principles.

References:

- [1] Cross J V, Walklate P J, Murray R A, Richardson G M.. Spray deposits and losses in different sized apple trees from an axial fan orchard sprayer: 1. Effects of spray liquid flow rate. *Crop Protection* 20, 13-30, 2001a.
- [2] Cross J V, Walklate P J, Murray R A, Richardson G M.. Spray deposits and losses in different sized apple trees from an axial fan orchard sprayer: 2. Effects of spray quality. *Crop Protection* 20 (4), 333-343, 2001b.
- [3] Cross J V, Walklate P J, Murray R A, Richardson G M.. Spray deposits and losses in different sized apple trees from an axial fan orchard sprayer: 3. Effects of air volumetric flow rate. *Crop Protection* 22, 381-394, 2003.
- [4] Prusinkiewicz P, Lindenmayer A.. *The algorithmic beauty of plants*. Springer Verlag, New York, 1990.

- [5] Salyani M, Wei J.. Effects of travel speed on characterizing citrus canopy structure with a laser scanner. *Precision Agriculture 05*. Edited by J.V. Stafford. Wageningen Academic Publishers. 185-192, 2005.
- [6] Sanz R, Palacin J, Siso JM, Ribes-Dasi M, Masip J, Arno J, Llorens J, Valles J M, Rosell J R.. Advances in the measurement of structural characteristics of plants with a LIDAR scanner. *Eur AgEng Conference*. Leuven. Paper NR 277, 2004.
- [7] Tarquis A, González-Andrés F.. Stochastic L-system Applied to the Calculation of the Leaf Area of a Shrubby Legume for Forage (*Chamaecytisus rathenicus*, F. ex Wol.). In: M.N. Novak (Editor), *Fractal Reviews in the Natural and Applied Sciences*, Chapman and Hall, 192-203, 1995.
- [8] Walklate P J, Richardson G M, Baker D E, Richards P A, Cross J V. . Short-range LIDAR measurement of top fruit tree canopies for pesticide application research in the UK. *Proceedings of the SPIE - International Society for Optical Engineering Advances in Laser Remote Sensing for Terrestrial and Oceanographic Application*, Orlando, Florida, 21-22 April 1997 3059, 143-151, 1997.
- [10] Walklate P J, Richardson G M, Cross J V, Murray R A. . Relationship between orchard tree crop structure and performance characteristics of an axial fan sprayer. *Aspects of Applied Biology* (57), Pesticide Application, Guildford, UK, 17-18 January 2000, 285-29, 2000.
- [11] Walklate P J, Cross J V, Richardson GM, Murray R A, Baker D E. 2002. Comparison of different spray volume deposition models using LIDAR measurements of apple orchards. *Biosystems Engineering* 82 (3), 253-267, 2002.
- [12] Walklate P J, Cross J V, Richardson G M, Baker D E, Murray R A.. A generic method of pesticide dose expression: Application to broadcast spraying of apple trees. *Annals of Applied Biology*, 143: 11-23, 2003.
- [13] Walklate P J, Tarquis, A.M., Méndez, V. and Lazzaro, L. . LIDAR simulation system based on trajectory model: estimation of spray target area. *Proceedings of International advances in pesticide application*, Cambridge University-U.K. , 2006.
- [14] Wangler RJ, Flower K L, McConnell II R E.. Object sensor and method for use in controlling an agricultural sprayer. U.S. Patent No. 5,278,323, United States Patent and Trademark Office, Washington, D.C., 1994.

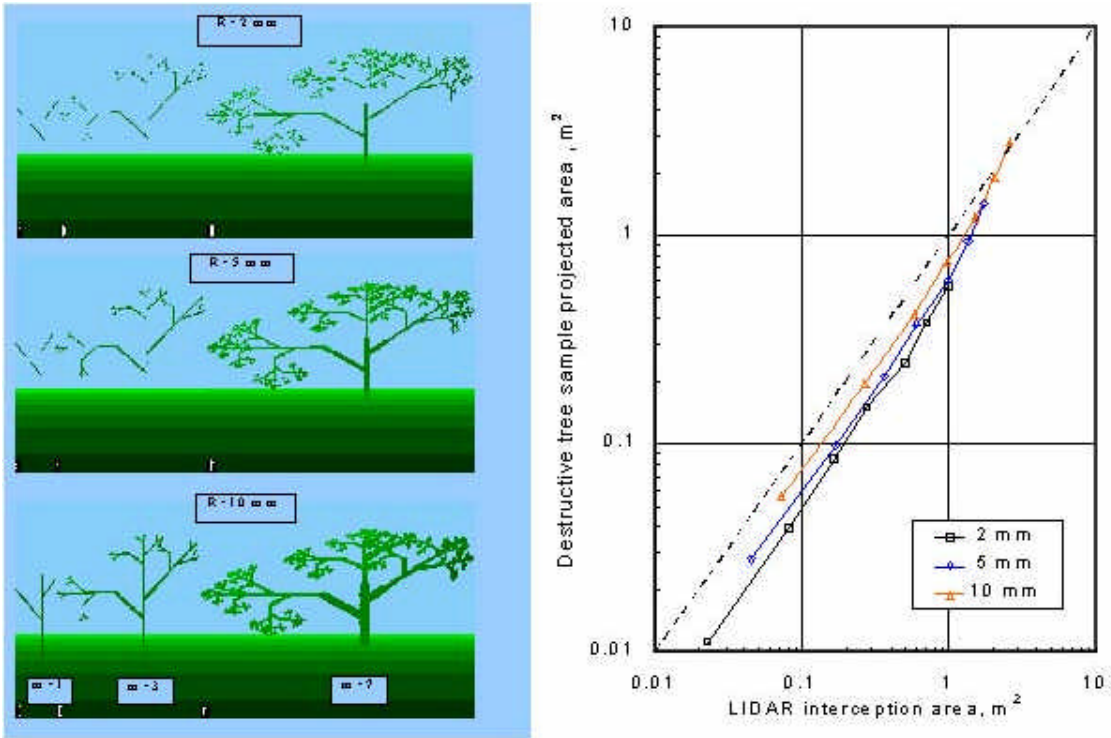


Fig. 2. Scaling effects of tree geometry obtained by perturbing the minimum branch radius at constant axiom rotation angle of 10° , vertical branching angle of 45° and branch element length of 0.4 m.

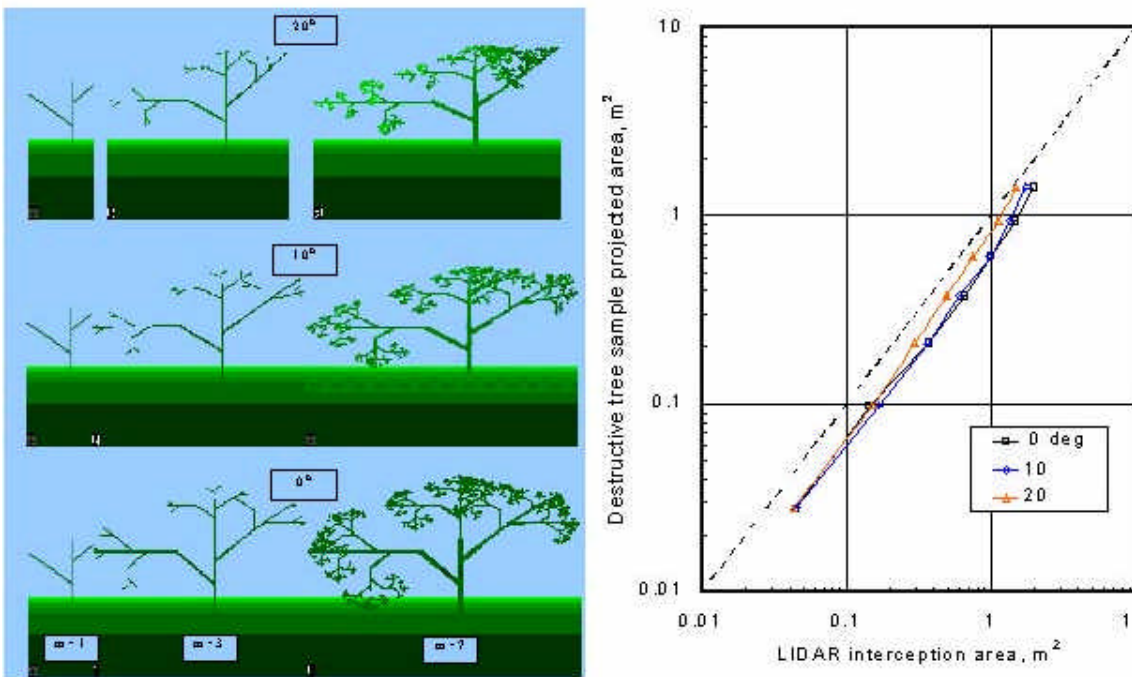


Fig. 3. Scaling effects of tree geometry obtained by perturbing the axiom rotation angle at constant minimum branch radius of 5 mm, vertical branching angle of 45° and branch element length of 0.4 m.

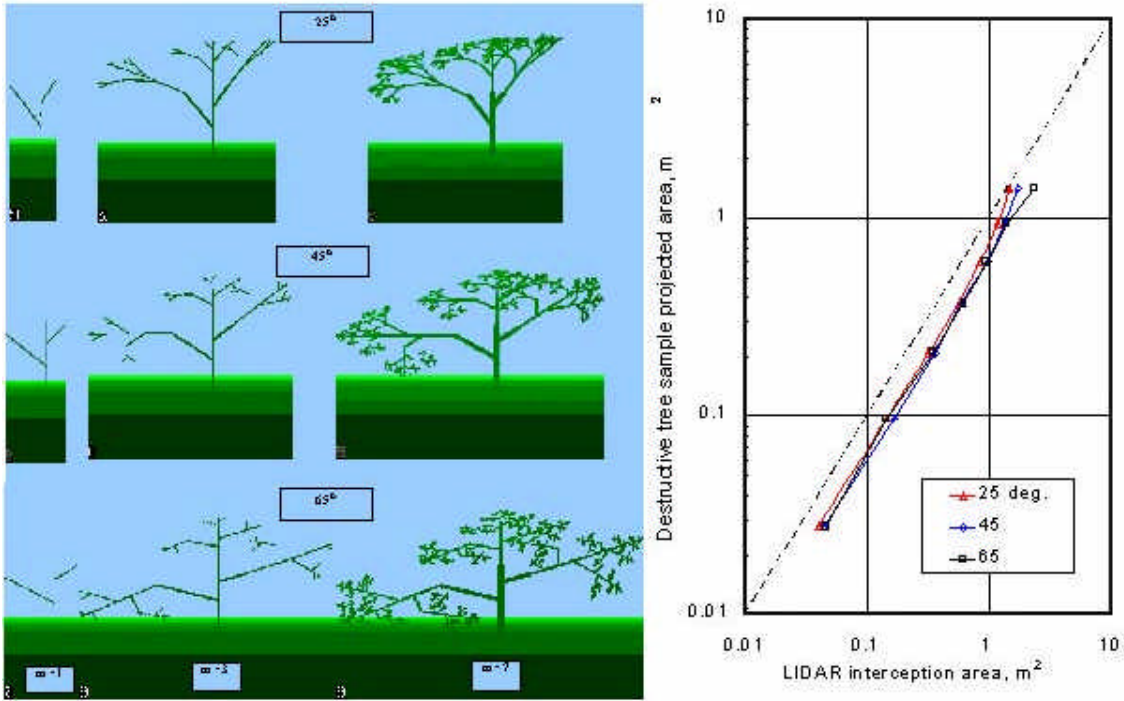


Fig. 4. Scaling effects of tree model geometry obtained by perturbing the vertical branching angle at constant minimum branch radius of 5 mm, axiom rotation angle of 100 and branch element length of 0.4 m.

